

Season and depth differences of soil moisture use for tree growth across wet and dry gradients in the Tibetan Plateau

Qian Li

Liang Jiao (✉ jjiaoliang@nwnu.edu.cn)

Northwest Normal University <https://orcid.org/0000-0001-6066-2346>

Ruhong Xue

Xichen Chen

Peng Zhang

Xuge Wang

Xin Yuan

Research Article

Keywords: Tree-ring oxygen isotopes, Wet and dry gradients, Water use dynamics, Spatial and temporal variation, Tibetan Plateau

Posted Date: August 23rd, 2023

DOI: <https://doi.org/10.21203/rs.3.rs-3236892/v1>

License: © ⓘ This work is licensed under a Creative Commons Attribution 4.0 International License. [Read Full License](#)

Abstract

Soil moisture has an important influence on tree growth in climate-sensitive regions. However, the seasonality of soil moisture utilization by trees in the Tibetan Plateau, a typical climate-sensitive region, and the mechanisms of depth of uptake are still unclear. Therefore, the spatial and temporal differences in the soil moisture use dynamics of tree growth were analyzed under wet and dry gradients on the Tibetan Plateau using tree-ring $\delta^{18}\text{O}$ ($\delta^{18}\text{O}_{\text{TR}}$). The results showed that: 1) soil moisture during the growing season was the main influencing factor on tree growth under different wet and dry gradients on the Tibetan Plateau. 2) The response of $\delta^{18}\text{O}_{\text{TR}}$ to soil moisture had a lag in arid areas than in wet areas. 3) In wet areas, trees absorbed the soil moisture in surface, while absorbed the soil moisture in deep in arid areas. And meanwhile, trees could develop more lateral and deep root systems using soil moisture from all soil layers to cope with climatic stress. In the future, more lateral and deep root systems of trees will be better suited to survive in complex habitats on the Tibetan Plateau, and that monitoring of trees in single water use areas should be enhanced. Further, it is of great significance to study soil water use strategies of tree growth under different wet and dry gradients for predicting forest ecosystem changes in complex environments.

1. Introduction

Global change affects tree adaptation in a variety of ways, leading to complex changes in forest ecosystem composition, structure and function, especially in the colder northern regions (Kenneth et al. 2022; Wang et al. 2023). Global changes in tree growth are largely attributed to interactions between temperature, precipitation and radiation balance (Seddon et al. 2016; Reichstein et al. 2017). In particular, the main factor influencing the growth of trees in humid environments is temperature, while the growth of trees in arid areas is mainly limited by moisture (Amer et al. 2023). Thus, there are differences in the sensitivity of tree growth to climate change under different wet and dry conditions.

Soil water is an important component of the water cycle that links the atmosphere, hydrosphere and biosphere, and is a major source of water for plants (Eslaminejad et al. 2020), which plays an important role in maintaining vegetation growth and ecosystem productivity. Soil moisture content varies with soil depth and season (Ma et al. 2020), and the water uptake mechanisms and adaptation strategies of trees to heterogeneous environments vary especially under different hydrological changes (Bertrand et al. 2014). The soil moisture was found to be the most important potential factors controlling the growth of vegetation on the Tibetan Plateau (Wang et al. 2018). The trees mainly use soil moisture during the growing season (Zeng et al. 2020; Zhang et al. 2022). However, it is important to note that the measurement and estimation of soil moisture is very complex and has great limitations for studying tree growth and water use strategies. Whereas tree rings can be used as a proxy for inversion of soil moisture changes on long time scales due to their continuous record, accurate dating, sensitivity to climate change, and wide distribution (Gao et al. 2018). For example, the oxygen isotopes in tree-ring have been used to reconstruct soil moisture in the western Himalayas over a period of nearly 100 years (Bose et al. 2016).

Due to the coupled processes of water uptake and transpiration by tree roots, interannual variation in tree-ring oxygen stable isotopes ($\delta^{18}\text{O}_{\text{TR}}$) can document seasonal changes in climate and the physiological-ecological response of trees to seasonal changes (Xu et al. 2020). Variations in $\delta^{18}\text{O}_{\text{TR}}$ are mainly influenced by $\delta^{18}\text{O}$ uptake of source water by growing trees, evaporative enrichment of leaf water, biochemical fractionation during photosynthesis, and xylem water exchange during the transport of carbohydrates to the trunk (Roden et al. 2000). This series of fractionation processes is regulated by external climate change (Brinkmann et al. 2019; Xiao et al. 2020). The $\delta^{18}\text{O}_{\text{TR}}$ are derived from soil water, which is ultimately derived from atmospheric water, mainly in relation to changes in precipitation, temperature and relative humidity (De et al. 2018). And changes in the atmospheric climate system are stored in soil moisture and are transferred to tree cellulose during the growing season to affect tree-ring oxygen isotopes. In addition, $\delta^{18}\text{O}_{\text{TR}}$ has the potential to reflect the depth of water uptake (Gessler et al. 2014). Variations in soil water $\delta^{18}\text{O}$ at different depths are preserved in the tree rings, but the strength of the soil water isotope signal preserved in the tree rings depends on the depth of water uptake by tree roots (Huang et al. 2019, Xu et al. 2020). In monsoon-controlled areas, precipitation $\delta^{18}\text{O}$ has a seasonal pattern and these signals are transmitted to various soil depths, causing soil water $\delta^{18}\text{O}$ to vary in vertical gradients with seasonal strength and direction (Lindh et al. 2014). Trees convert the isotopic composition of source water to the isotopic composition of cellulose through complex non-linear physicochemical processes (Ballantyne et al. 2016). For example, it has been shown that trees in the East Asian monsoon zone significantly correlated with soil moisture during the growing season, but the seasonal response was earlier in wet areas than in dry areas, and wet areas used mainly shallow soil water while dry areas used deep soil water (Wang et al. 2021). However, other study also showed trees in the East Asian monsoon region used deep water in the dry season and shallow soil water in the non-dry season (Yang et al. 2015). Therefore, there is uncertainty in the study of water use strategies based on $\delta^{18}\text{O}_{\text{TR}}$.

Controlled by the Asian monsoon, the climate of the Tibetan Plateau has undergone some changes in recent years, mainly including increasing surface temperatures (Sun et al. 2022), weakening monsoons (Wong et al. 2020) and reduced potential evaporation (Fang et al. 2019) since the 1960s. Changes in summer wind activity affect monsoon precipitation by altering the spatial pattern of regional water vapor transport, ultimately leading to interannual variability in $\delta^{18}\text{O}_{\text{TR}}$ (Ge et al. 2017; Tan et al. 2018). However, current studies on the Tibetan Plateau based on $\delta^{18}\text{O}_{\text{TR}}$ have mainly focused on climate reconstruction (Grießinger et al. 2019; Xu et al. 2019) and physiological mechanisms (Zhang et al. 2018). Therefore, this study aims to address three main questions: (1) whether there are differences in the seasonal dynamics of tree water use under different wet

and dry gradients on the Tibetan Plateau, (2) whether there are differences in the ability of tree growth to use water at different soil depths under different wet and dry gradients, (3) and what are the combined adaptation mechanisms of trees based on the seasonal dynamics and soil depth of tree water use under different wet and dry gradients?

2. Materials and methods

2.1 Study areas

The six sites in the Tibetan Plateau were selected for the study such as Delingha region (DE), the Ganesh (GA) and Wache (WA) regions in the south, the Manali (MA) and Jageshwar (JA) regions in the southwest, and the Karakorun (KA) region in the west (Fig. 1). Except for the KA region which is affected by the westerly winds and the other regions are affected by the Asian summer winds. From the wettest JA region to the driest DE region, the annual precipitation decreased by 1,311 mm (Fig.S1). The six regions are divided into humid and arid areas based on annual precipitation. Specifically, the humid areas include the JA, WA and GA regions, while the arid areas include the MA, KA and DE regions.

Please insert **Fig. 1** about here.

2.2 Tree-ring isotope data

The $\delta^{18}\text{O}_{\text{TR}}$ data in this study were downloaded from NOAA Paleoclimatology Datasets (<https://www.ncsl.noaa.gov/pub/data/paleo/tree-ring/isotope/asia>). These $\delta^{18}\text{O}_{\text{TR}}$ chronologies are common to the years 1948–1998, and the specific locations, elevations, tree species, and $\delta^{18}\text{O}_{\text{TR}}$ chronological lengths of the sampled sites were shown in Table 1. The sampling sites were largely located in high-elevation areas, and all of the selected tree species were conifers. Tree cores were collected at breast height using increment borers. And alpha-cellulose extraction process included chemical reactions with organic reagents, sodium chlorite and sodium hydroxide to remove extractions (ash, resin, etc.), lignin and hemicellulose, respectively (Shi et al. 2015). Elevation gradients and age differences in the plateau had no significant effect on the climatic response of $\delta^{18}\text{O}_{\text{TR}}$ records (Wernicke et al. 2015; Zeng et al. 2016).

Please insert **Table 1** about here.

Table 1
Chronological information on tree rings

Sites	Location	Elevation	Species	period	Rbar	Date Source
JA	29°38'N, 79°51'E	1870m	<i>Cedrus deodara</i>	1621–2008	0.61–0.78	Xu et al (2018)
WA	27°59'N, 90°00'E	3500m	<i>Larix griffithii</i>	1743–2011	0.74–0.88	Sano et al (2013)
GA	28°10'N, 85°11'E	3500m	<i>Abies spectabilis</i>	1801–2000	0.56–0.78	Xu et al (2018)
MA	32°13'N, 77°13'E	2700m	<i>Abies pindrow</i>	1768–2008	0.71–0.92	Sano et al (2017)
KA	35°54'N, 74°56'E	2900m	<i>Juniperus excelsa</i>	1990–1998	0.51	Treydte et al (2006)
DE	37°48'N, 97°78'E	3500m	<i>Juniperus przewalskii</i>	-4680-2011	0.40–0.76	Yang et al (2021)

2.3 Meteorological data

Our meteorological data included the maximum, mean and minimum temperatures, actual vapor pressure, and precipitation and the Palmer drought severity index (PDSI) on monthly-scale for six regions (Fig.S1). The grid point data above were obtained from Climate Explorer (<http://climexp.knmi.nl/start.cgi>). Since saturation water vapor pressure deficit (VPD) and relative humidity (RH) data for the region are difficult to obtain, we calculated VPD (Murray 1966) and RH (New et al. 1999) based on the downloaded CRU TS4.04 (0.5°×0.5°) dataset, and the specific calculation procedure as follows:

$VPD = \text{actual water vapour pressure} - \text{saturated water vapour pressure} = e^0 \times 10^{\left(\frac{T}{5.237.3}\right)} - \text{actual water vapour pressure}$	(Eq. 1)
$RH = \left(\frac{e}{e_{sat}}\right) \times 100$	(Eq. 2)
$e_{sat} = 6.108 \times \exp(17.27 \times T / (T + 273.3))$	(Eq. 3)

In the above equation, $e^0 = 6.11 \text{ hpa}$, T is the monthly mean temperature (unit: °C).

2.4 Soil moisture data

Soil moisture data were obtained from the Global Land Data Assimilation System (<http://ldas.gsfc.nasa.gov/gldas>) with a temporal resolution of 1948–2015 and a spatial resolution of $0.25^\circ \times 0.25^\circ$. This dataset has a longer temporal resolution and a higher resolution for soil moisture at different depths compared to other datasets. We selected soil moisture data from 1948–1998 at three depths with 0–10cm, 10–40cm and 40–100cm for our study. The soil moisture data we downloaded (unit: kg/m^2) had to be further converted to volumetric water content (VWC, unit: m^3/m^3) for data analysis by the following conversion equation:

$$VWC = \frac{\text{kg} \times 1000}{\text{m}^2 \times 1000 \text{ kg/m}^3} \times \frac{1}{\text{thickness of layer in mm}} \quad (\text{Eq. 4})$$

2.5 Data Analysis

To investigate the elements of environmental factors that mainly affect $\delta^{18}\text{O}_{\text{TR}}$, we used Pearson correlation as well as partial correlation analysis. In the meanwhile, One-way analysis of variance (ANOVA) was used to assess the variability of the $\delta^{18}\text{O}_{\text{TR}}$ chronology and the significance of differences was tested using Tukey's multiple comparisons. Spatial correlation analysis was performed using Matlab 2023 and mapped using ArcGIS 10.8.

3. Results

3.1 Comparison of the spatial and temporal dynamics of $\delta^{18}\text{O}_{\text{TR}}$ under the wet and dry gradients

Please insert Fig. 2 about here.

The spatial dynamics of $\delta^{18}\text{O}_{\text{TR}}$ showed an overall higher value in the north and lower value in the south (Fig. 3). The lowest value of $\delta^{18}\text{O}_{\text{TR}}$ occurs in the southern part of the plateau (WA, 19.401‰) and the highest value is located in the northeastern part of the plateau (DE, 32.907‰). The value of $\delta^{18}\text{O}_{\text{TR}}$ decreased as the climate changed from arid to humid areas.

Please insert Fig. 3 about here.

3.2 Comparison of the spatial and temporal dynamics of soil water content patterns at different depths under wet and dry gradients

Soil water content at different gradients on the Tibetan Plateau showed inconsistent soil depth variation characteristics and temporal dynamics (Fig. 4). Specifically, the soil water content in the six gradient regions showed the increasing trends with increasing soil depth from 0–10 cm, 10–40 cm to 40–100 cm (Fig. 4a). At the same time, the soil moisture content in the wet areas was significantly greater than that in the arid areas, accompanied by a greater variation in moisture content ($VWC_{\text{JA, WA, GA}} > VWC_{\text{MA, KA, DE}}$), especially in the DE area, where the moisture content of all soil layers is lower than in the other areas.

In terms of time, the seasonal dynamics of soil moisture content were more pronounced in the wetter areas than in the arid areas (Fig. 4b), where the peak soil moisture content was mainly concentrated in June–September. The volumetric water content from July to September was 48.9% (JA), 49.1% (WA) and 47.8% (GA) of the year, respectively. However, the seasonal dynamics of soil moisture content in the arid areas varied more between regions. In the MA region with the double-peaked model, the volumetric water content from June to September accounts for 32.8% of the year. However, the high values of volumetric water content in the KA region are concentrated in April–June, accounting for 32.3% of the year. But no seasonal dynamic peaks in soil moisture content were formed in the driest DE region.

Please insert Fig. 4 about here.

The moisture content of each soil layer in the humid areas was significantly greater than in the arid areas and decreases significantly with the decrease in regional precipitation (Fig. 5). Specifically, in the humid areas, the soil moisture in each soil layer in each regions tends to decrease and the most significant decrease was in the 40–100 cm range. In the arid areas, soil moisture showed an overall increasing trend, but the MA area shows a decreasing trend in all soil layers, which is closely related to the weakening of the monsoon in the region and the decrease in precipitation. Meanwhile, the linear fit of precipitation to soil moisture was stronger in the wetter regions than in the arid regions, with the fit becoming progressively worse from the wettest JA region to the driest DE region (Fig. S2).

Please insert Fig. 5 about here.

3.3 Comparison of $\delta^{18}\text{O}_{\text{TR}}$ response to climatic and soil moisture factors under wet and dry gradients

It is revealed that overall $\delta^{18}\text{O}_{\text{TR}}$ responded negatively to PDSI, precipitation and RH, and positively to temperature and VPD in different humid and arid areas (Fig. 6). However, seasonal response differences were observed in humid and arid environments, showing $\delta^{18}\text{O}_{\text{TR}}$ more often correlated with environmental factors in the middle of the growing season (June-August) in humid environments, and with environmental factors in the middle and late growing season (July- September) in arid areas.

Further, comparing the responses of $\delta^{18}\text{O}_{\text{TR}}$ to soil water content at different soil depths in humid and arid areas showed variability in depth as well as time (Fig. 7). In general, the correlation was greater in wet areas with 0–10 cm and 10–40 cm in July ($p < 0.01$), while the arid environment $\delta^{18}\text{O}_{\text{TR}}$ was significantly negatively correlated with soil moisture in 10–40 cm and 40–100 cm soil layers in September ($p < 0.01$). The seasonal response of $\delta^{18}\text{O}_{\text{TR}}$ to soil moisture was lagged in the dry areas compared to the humid areas. Specifically, in humid areas, $\delta^{18}\text{O}_{\text{TR}}$ was significantly negatively correlated with 0–40 cm soil moisture in July and August in JA and WA ($r = -0.49$ to -0.41 , $p < 0.05$), while $\delta^{18}\text{O}_{\text{TR}}$ in GA region was significantly negatively correlated with soil moisture at all three soil depths ($r = -0.44$ to -0.26 , $p < 0.05$). However, in arid environments, $\delta^{18}\text{O}_{\text{TR}}$ was significantly negatively correlated with soil moisture at all three soil depths from July to September in MA ($r = -0.47$ to -0.31 , $p < 0.05$), while $\delta^{18}\text{O}_{\text{TR}}$ in KA and DE regions were more significantly negatively correlated with soil moisture at 40–100 cm from July to September ($r = -0.48$ to -0.29 , $p < 0.05$).

Please insert Fig. 6 about here.

3.4 Correlation between $\delta^{18}\text{O}_{\text{TR}}$ and key environmental factors during the growing season from June to September under the wet and dry gradients

The correlation between $\delta^{18}\text{O}_{\text{TR}}$ and soil moisture during the growing season (June-September) was found to be significantly stronger than other environmental variables through Pearson correlation analysis. Therefore, we further selected key environmental factors that strongly influenced $\delta^{18}\text{O}_{\text{TR}}$ in different regions during the growing season for a partial correlation analysis (Table 2). The results showed that when VPD and RH were controlled, $\delta^{18}\text{O}_{\text{TR}}$ was significantly negatively correlated with 0–10 cm soil moisture in the wet environment in JA ($p < 0.05$), while it was significantly correlated with 0–10 cm and 10–40 cm soil moisture in WA and GA ($p < 0.05$). When VPD and RH were controlled, $\delta^{18}\text{O}_{\text{TR}}$ was highly significantly negatively correlated with soil moisture at all soil depths in MA ($p < 0.01$), while $\delta^{18}\text{O}_{\text{TR}}$ was significantly negatively correlated with soil moisture at 40–100 cm in KA and DE ($p < 0.05$).

Please insert Fig.7 about here.

Table 2
Partial correlation analyzes between $\delta^{18}\text{O}_{\text{TR}}$ and environmental factors from June-September.

Control variables	Correlations with $\delta^{18}\text{O}_{\text{TR}}$	JA	WA	GA	MA	KA	DE
VPD	VMC ₀₋₁₀	-0.396	-0.364	-0.409	-0.459	-0.211	-0.145
	VMC ₁₀₋₄₀	-0.265	-0.36	-0.383	-0.472	-0.277	-0.286
	VMC ₄₀₋₁₀₀	-0.21	-0.225	-0.241	-0.416	-0.356	-0.385
PDSI	PDSI	-0.161	-0.106	-0.255	-0.264	-0.278	-0.585
	RH	0.27	0.179	0.423	0.151	-0.064	-0.163
	VMC ₀₋₁₀	-0.251	-0.459	-0.365	-0.527	-0.004	0.173
PDSI	VMC ₁₀₋₄₀	-0.213	-0.451	-0.317	-0.542	-0.118	0.164
	VMC ₄₀₋₁₀₀	-0.14	-0.156	-0.343	-0.5	-0.239	0.119
	VPD	0.057	0.432	-0.141	-0.314	0.003	-0.021
RH	RH	0.072	-0.396	0.251	-0.028	-0.042	-0.022
	VMC ₀₋₁₀	-0.356	-0.377	-0.392	-0.53	-0.213	-0.13
	VMC ₁₀₋₄₀	-0.289	-0.38	-0.365	-0.542	-0.276	-0.274
RH	VMC ₄₀₋₁₀₀	-0.214	-0.225	-0.28	-0.499	-0.352	-0.365
	VPD	0.296	0.259	0.367	0.159	-0.042	-0.008
	PDSI	-0.208	-0.113	-0.242	-0.315	-0.277	-0.57

Note: * and ** indicated $p < 0.05$ and $p < 0.01$, respectively. The VMC₀₋₁₀ represents the volume moisture content of 0-10cm soil, the VMC₁₀₋₄₀ represents the volume moisture content of 10-40cm soil, he VMC₄₀₋₁₀₀ represents the volume moisture content of 40-100cm soil.

Please insert **Table 2** about here

3.5 Comparison of spatial characteristics of $\delta^{18}\text{O}_{\text{TR}}$ response to soil moisture content at different soil depths under wet and dry gradients

The spatial correlation analysis revealed that the response of $\delta^{18}\text{O}_{\text{TR}}$ to soil moisture at all six sites in the study area was generally negatively correlated. But the overall differences in the responses of $\delta^{18}\text{O}_{\text{TR}}$ to soil moisture content at 0–10 cm and 10–40 cm were not significant, and the significant difference was found at 40–100 cm (Fig. 8). And the responses of $\delta^{18}\text{O}_{\text{TR}}$ to soil moisture in the southern and northeastern parts of the plateau changed from negative to positive as the soil depth deepened (Fig. 8). Specifically, $\delta^{18}\text{O}_{\text{TR}}$ was negatively correlated with soil moisture at 0–10 cm of all sites. But the correlation showed a trend of JA > WA > GA > MA > KA > DLH. That is, the drier the climate, the lower the correlation between $\delta^{18}\text{O}_{\text{TR}}$ and soil moisture at 0–10 cm and 10–40 cm. However, the positive responses of $\delta^{18}\text{O}_{\text{TR}}$ to soil moisture at the depth of 40–100 cm increases in DE of the northeastern part and in WA of the south.

Please insert **Fig.8** about here.

4 Discussion

4.1 The $\delta^{18}\text{O}_{\text{TR}}$ records soil water use by tree growth in different regions of the Tibetan Plateau

Since the 1960s, the surface temperature of the Tibetan Plateau has shown a continuous warming trend (Duan et al. 2015), and precipitation has increased in the western and eastern parts of the plateau (Bao et al. 2019; Liu et al. 2020), but weakened in the southwestern part of the plateau (Hu et al. 2021). In such a climatic change context, trees may adopt different water use strategies to maintain their growth. It has been shown that $\delta^{18}\text{O}_{\text{TR}}$ could reflect the seasonality and the depth of plant water uptake (Gessler et al. 2014). This means that information on the variation of soil water $\delta^{18}\text{O}$ at different seasons and depths is stored and recorded in the tree-ring (Huang et al. 2019, Xu et al. 2020).

The $\delta^{18}\text{O}_{\text{TR}}$ variations are mainly regulated by a combination of the oxygen isotope composition of the source water, and the external climate that affects fractionation processes within the tree (Roden et al. 2000). In our results, the $\delta^{18}\text{O}_{\text{TR}}$ was more sensitive to moisture factors than to temperature factors, and in particular $\delta^{18}\text{O}_{\text{TR}}$ showed the significant negative response to soil moisture during the growing season (Fig. 5). The $\delta^{18}\text{O}_{\text{TR}}$ is derived from soil water, but that soil water $\delta^{18}\text{O}$ varies with soil depth (Liu et al. 2017), which is consistent with our findings. In addition, water enters the leaves from the soil through the xylem and then the lighter isotope (^{16}O) evaporates more readily than the heavier isotope (^{18}O), leading to an enrichment of $\delta^{18}\text{O}$ in leaf water (Farquhar et al. 1993). Trees take up soil water directly through the root system and retain the isotopic signal in soil water in the xylem through a series of intra-tree fractionation processes. Therefore, the $\delta^{18}\text{O}_{\text{TR}}$ is a true reflection of soil water use by trees based on the processes of water uptake, transport and dissipation in trees.

At the same time, our study found that $\delta^{18}\text{O}_{\text{TR}}$ values were significantly greater in arid than in humid areas (Fig. 3), due to the fact that transpiration affects leaf water enrichment by replenishing unenriched soil water to the leaves. On the one hand, the $\delta^{18}\text{O}_{\text{TR}}$ is mainly negatively correlated with stomatal conductance, and reduced soil moisture and humidity enhance evaporative enrichment of leaf and soil water through effects on stomatal conductance and the ratio of internal leaf CO_2 to atmospheric CO_2 in arid environments (Mirfenderesgi et al. 2016). On the other hand, soil water evaporation is enhanced in arid environments and the source water absorbed by tree roots becomes heavier, leading to an enrichment of oxygen isotopes in leaf water (Roden et al. 2000). Sucrose produced by photosynthesis is transported through the bast to the xylem of the trunk for cellulose synthesis, and during the conversion to cellulose, oxygen isotopes in the sugar are partially exchanged with oxygen isotopes in the source water (Zhan et al. 2021), resulting in a mixed signal of both source water and transpiration-enriched oxygen isotopes in the cellulose oxygen isotope ratio of the tree-ring (Giraldo et al, 2022). These two processes result in a higher $\delta^{18}\text{O}_{\text{TR}}$ in arid areas than in humid areas. Similarly, a moist atmosphere reduces transpiration and thus ^{18}O water enrichment in needles, further leading to lower $\delta^{18}\text{O}_{\text{TR}}$ in humid areas than in arid areas. And precipitation $\delta^{18}\text{O}$ is inversely related to precipitation, more precipitation leads to lower precipitation $\delta^{18}\text{O}$ values, resulting in weaker $\delta^{18}\text{O}$ enrichment of water from water sources absorbed by trees, both of which make $\delta^{18}\text{O}_{\text{TR}}$ in wet areas lower than in arid areas (Yang et al. 2012).

4.2 Difference strategies of season in soil moisture use dynamics for tree growth under different wet and dry gradients on the Tibetan Plateau

In climate-sensitive areas, soil moisture is critical to tree growth. A variety of factors can alter soil water uptake by trees, such as season (Rao et al. 2020), life history stage (Van et al. 2017), tree species (Schwendenmann et al. 2015), water availability and depth of plant access to water (Rao et al., 2020), and the amount of recent rainfall (Xu et al. 2011). In our study, $\delta^{18}\text{O}_{\text{TR}}$ was found to be significantly correlated with soil moisture during the growing season, but the seasonal response in arid and wet zones showed inconsistency, with tree-ring $\delta^{18}\text{O}$ responding to soil moisture later in arid zones than in wet zones (Fig. 7).

Specifically, in the humid areas, we found that $\delta^{18}\text{O}_{\text{TR}}$ significantly negatively correlated with soil moisture from June to August ((Fig. 7). Because the three humid regions are influenced by the Indian summer winds and receive more precipitation from June to August, which further affects $\delta^{18}\text{O}_{\text{TR}}$ by influencing soil water ^{18}O through infiltration. The JA and GA regions showed a significant negative correlation between $\delta^{18}\text{O}_{\text{TR}}$ and July-September precipitation, Indian monsoon index, and monsoon circulation intensity in the region (Xu et al. 2018). And we also found a significant negative correlation between $\delta^{18}\text{O}_{\text{TR}}$ and soil moisture during July-August in JA and GA regions. And meanwhile, $\delta^{18}\text{O}_{\text{TR}}$ values of different tree species in the WA region were mainly influenced by summer precipitation since 1743 (Masaki et al. 2012). In our study, we also found that $\delta^{18}\text{O}_{\text{TR}}$ in the WA region was significantly negatively correlated with soil moisture in July and August. We suggest that summer winds bring abundant precipitation, and that plant roots take up water in the soil through a series of transpiration infiltration processes, finally retaining the isotopic signal of precipitation in the xylem of trees expressed through $\delta^{18}\text{O}_{\text{TR}}$ in humid regions.

We also found the response of $\delta^{18}\text{O}_{\text{TR}}$ in arid regions significantly correlated with soil moisture from July to September, especially in September (Fig. 7). But the response of $\delta^{18}\text{O}_{\text{TR}}$ to soil moisture in arid regions was lagged compared to wet regions, which may be closely related to the extended growing season of trees due to warming and humidification of the Tibetan Plateau in recent decades (Zhang et al. 2021). However, the specific response varied among the three arid regions. The $\delta^{18}\text{O}_{\text{TR}}$ in the MA region was controlled by hydroclimatic variables such as summer monsoon precipitation, RH and PDSI (Masaki et al. 2017). Those results suggesting that monsoon precipitation has a significant effect on tree growth. Tree growth in the KA region is mainly influenced by winter snowfall, and although trees are still affected by precipitation $\delta^{18}\text{O}$ during summer precipitation, the melting snowfall provides a more stable water source, resulting in a much lower correlation between $\delta^{18}\text{O}_{\text{TR}}$ and summer soil moisture in this region than in the other two regions (Kerstin et al. 2006). In the driest DE region, the $\delta^{18}\text{O}_{\text{TR}}$ were controlled mainly through soil moisture and precipitation variability from May to September (Yang et al. 2006), and our study provided further evidence that $\delta^{18}\text{O}_{\text{TR}}$ in this region was significantly negatively correlated with soil moisture in September.

In the meantime, it has been found that precipitation has a greater effect on soil moisture than temperature on the southeastern Tibetan Plateau. Soil moisture is significantly correlated with oxygen isotope growing season in the southeastern Tibetan Plateau trees (Wang et al. 2023). And the $\delta^{18}\text{O}_{\text{TR}}$ were found to be significantly negatively correlated with growing season precipitation in the United Kingdom (Giles et al. 2015), southern Mexico (Brienen et al. 2013), northwestern Tibetan Plateau (Zhang et al. 2021), and Ordos Plateau (Li et al. 2019), which was broadly in line with our findings that summer rainfall to supplement plant water availability during the growing season (Hahm et al. 2019). We speculated that this were two reasons for the lagging response of $\delta^{18}\text{O}_{\text{TR}}$ to soil moisture in arid areas relative to humid areas. On the one hand, it might be because the Indian summer winds, which firstly reached the southern region, making precipitation events occur earlier in the southern region in their northward push. Therefore, they affect the tree growth process through a series of fractionation as well as plant physiological processes, then reflecting different moisture. On the other hand, this is closely related to the warming and humidification in the western and northern parts of the plateau, where warmer temperatures and increased precipitation lead to an earlier and longer growing season for trees. Moreover, precipitation in early in the growing season was not replenished in time, while both precipitation and temperature at the end of the growing season promoted tree growth, making the response of $\delta^{18}\text{O}_{\text{TR}}$ to soil moisture slightly later in the arid areas than in the humid areas (Guo et al. 2022).

4.3 Difference strategies of depth in soil moisture use dynamics for tree growth under different wet and dry gradients on the Tibetan Plateau

Precipitation on the Tibetan Plateau, where the natural environment is extremely fragile and sensitive, is highly spatially variable with annual precipitation decreasing gradually with latitude (Li et al. 2022). Therefore, trees might maintain their growth by altering their water use strategies to absorb soil moisture at different depths under different precipitation conditions. Most studies have shown that trees in arid environments tend to absorb deeper water to resist drought (Hu et al. 2021), whereas trees in wet environments tended to use shallow soil water (Holdo et al. 2018). While this was supported in our study, we have also found that trees in complex climatic environments may develop complex root systems with both lateral and deep roots, adjusting their water use strategies to maintain their growth in response to environmental changes.

Our study also found that, the $\delta^{18}\text{O}_{\text{TR}}$ in the JA region was significantly negatively correlated with 0–10 cm soil moisture in a wet environment, while that in the WA and GA regions were significantly negatively correlated with 0–10 cm and 10–40 cm soil moisture after controlling the VPD and RH (Table 2), it suggesting that trees in humid areas tended to take up soil moisture in the surface and middle layers. Other studies also found shallow soil water (35%) and precipitation (32.5%) were the main sources of water for trees in wet areas when annual precipitation was greater than 800 mm (Zhou et al. 2011). Meanwhile, the topsoil in humid areas is the most active area for microbial activity, so that it provides nutrients to the trees (Priyadarshini et al. 2016). For example, it has been shown that trees had a relatively large range of source water and a good water use strategy in the shallow soil under humid climate conditions (Sun et al. 2019).

In arid environments, the significant negative correlation between $\delta^{18}\text{O}_{\text{TR}}$ and 40–100 cm soil moisture in the KA and DE regions was revealed after controlling VPD and RH (Table 2), it suggesting that trees in arid environments utilize more stable deep soil moisture. And trees in DE region preferred to take up deep soil moisture through a study of cypress in the northeastern Tibetan Plateau (Grossiord et al. 2016), which validates our results. In arid environments, capillary water induces trees to form deeper root systems to absorb deep soil water and groundwater to meet higher transpiration needs during the dry season, while deep root systems provide a more consistent and reliable source of water for trees (Lindh et al. 2014). But we also found the highly significant negative correlations between $\delta^{18}\text{O}_{\text{TR}}$ and soil moisture at all soil depths in MA, and there might be two factors. On the one hand, soil moisture $\delta^{18}\text{O}$ fractionation occurs when precipitation infiltrates into the soil (Oerter et al. 2014), creating an isotopic gradient in the vertical profile while vigorous evaporation may mask some of the isotopic signal (Dai et al. 2015). On the other hand, it is possible that the 'bimodal' precipitation pattern in this region encourages trees to develop lateral and deep root systems, using the surface root system to obtain water from the upper soil layer when precipitation is adequate. The deep root system is used to obtain water from deep soil or groundwater when precipitation is insufficient (Zhang et al. 2017). This confirms our finding that trees adjust their water use strategies in time to sustain self-sustaining growth (Zhao et al. 2018; Nolan et al. 2018).

Trees under different environmental conditions have different coping strategies to climate extremes, and the resilience of trees to drought is closely related to regional soil moisture, diurnal temperature differences, and plant physiological characteristics (Fang et al. 2018). It has been reported that tree growth on the Tibetan Plateau is more vulnerable to challenges in the context of climate change (Zhang et al. 2021; Yao et al. 2023). Our results suggest that trees in arid areas are better able to cope with drought stress due to their use of more stable deep soil water, whereas trees in humid areas may be more vulnerable to drought stress in the context of climate variability due to their use of surface-middle soil water. As a result, trees in wetter areas will face greater challenges to survival in the context of a weakening southwestern monsoon with reduced precipitation and continued warming temperatures. Moreover, it is noteworthy that trees develop the water use strategy of absorbing moisture from different soil layers with the stronger lateral and deep root systems as the environment changes, which can more be beneficial to trees in coping with complex environment.

5. Conclusion

The climate of the Tibetan Plateau has changed significantly in recent decades. It is of great significance to study the water use strategies of trees in this region for monitoring its ecological environment. Therefore, the relationship between oxygen isotope data and environmental factors in tree

ring on the Tibetan Plateau were investigated. We found that $\delta^{18}\text{O}_{\text{TR}}$ recorded spatial and temporal differences in soil moisture use dynamics by tree growth under different wet and dry gradients. Our results showed that $\delta^{18}\text{O}_{\text{TR}}$ responded more strongly to soil moisture than other environmental factors during the growing season under different wet and dry gradients, but the response in the arid areas had a lag compared to the humid areas. Meanwhile, trees in the humid southwestern region absorbed more shallow soil water, while trees in the arid western and northeastern regions absorbed more deep soil water. We suggest that trees use shallow soil water alone increase the risk of drought stress in a southwestern context of decreasing precipitation and increasing temperatures, whereas trees develop both lateral and deep root systems are better able to survive in complex environments. As a water tower in Asia, the Tibetan Plateau has an important influence on the climate of the Northern Hemisphere. We recommend the use of this method for larger-scale and more regional studies to research the response strategies of trees and ecological changes in the context of climate change.

Declarations

Acknowledgments

We would like to thank the colleagues in the Northwest Normal University for their help in the writing process. We are grateful to anonymous reviewers and editorial staff for their constructive and helpful suggestions.

Funding

This research was supported by CAS "Light of West China" Program (2020XBZG-XBQNxz-A), Basic Research Innovation Group Project of Gansu Province (No. 22JR5RA129), and the 2022 Major scientific Research Project Cultivation Plan of Northwest Normal University (WNU-LKZD2022-04). We also thank the anonymous referees for helpful comments on the manuscript.

Conflicts of Interest

The authors declare no conflict of interest.

Data Availability Statement

All data sources analyzed in this study are included in this paper.

References

1. Amer A, Franceschi E, Hjazin A (2023). Structure and Ecosystem Services of Three Common Urban Tree Species in an Arid Climate City. *Forests* 14(4): 671
2. An W., Hou S, Zhang Q, Zhang W, Wu, S, Xu H, Liu Y (2017) Enhanced recent local moisture recycling on the northwestern Tibetan Plateau deduced from ice core deuterium excess records. *Journal of Geophysical Research: Atmospheres* 122(23): 12-541
3. Anchukaitis KJ (2017) Tree rings reveal climate change past, present, and future. *Proceedings of the American Philosophical Society* 161(3): 244-263
4. Anderson MC, Allen RG, Morse A, Kustas P (2012) Use of Landsat thermal imagery in monitoring evapotranspiration and managing water resources. *Remote Sensing of Environment* 122: 50-65
5. Baker JCA, Gloor M, Spracklen DV, Arnold SR, Tindall JC, Clerici SJ, Brienen RJW (2016) What drives interannual variation in tree ring oxygen isotopes in the Amazon. *Geophysical Research Letters* 43(22): 11-831
6. Bershaw J, Penny SM, Garzione CN (2012) Stable isotopes of modern water across the Himalaya and eastern Tibetan Plateau: Implications for estimates of paleoelevation and paleoclimate. *Journal of Geophysical Research: Atmospheres* 117(D2)
7. Bertrand G, Masini J, Goldscheider N, Meeks J, Lavastre V, Celle-Jeanton H, Hunkeler D (2014) Determination of spatiotemporal variability of tree water uptake using stable isotopes ($\delta^{18}\text{O}$, $\delta^2\text{H}$) in an alluvial system supplied by a high-altitude watershed, Pfyn forest, Switzerland. *Ecohydrology* 7(2): 319-333
8. Bose T, Sengupta S, Chakraborty S, Borgaonkar H (2016) Reconstruction of soil water oxygen isotope values from tree ring cellulose and its implications for paleoclimate studies. *Quaternary International* 425: 387-398
9. Brienen RJ, Hietz P, Wanek W, Gloor M (2013) Oxygen isotopes in tree rings record variation in precipitation $\delta^{18}\text{O}$ and amount effects in the south of Mexico. *Journal of Geophysical Research: Biogeosciences* 118(4): 1604-1615
10. Brinkmann N, Eugster W, Buchmann N, Kahmen A (2019) Species-specific differences in water uptake depth of mature temperate trees vary with water availability in the soil. *Plant Biology* 21(1): 71-81

11. Dai Y, Zheng XJ, Tang LS, Li Y (2015) Stable oxygen isotopes reveal distinct water use patterns of two *Haloxylon* species in the Gurbantonggut Desert. *Plant and Soil* 389: 73-87
12. De Deurwaerder H, Hervé-Fernández P, Stahl C, Burban B, Petronelli P, Hoffman B, Verbeeck H (2018) Liana and tree below-ground water competition—evidence for water resource partitioning during the dry season. *Tree physiology*, 38(7), 1071-1083
13. Ding J, Cuo L, Zhang Y, Zhu F (2018) Monthly and annual temperature extremes and their changes on the Tibetan Plateau and its surroundings during 1963–2015. *Scientific reports* 8(1): 1-23
14. Duan A, Xiao Z (2015) Does the climate warming hiatus exist over the Tibetan Plateau? *Scientific reports* 5(1): 13711
15. Eslaminejad P, Heydari M, Kakhki FV, Mirab-balou M, Omidipour R, Muñoz-Rojas M, Lucas-Borja M E (2020). Plant species and season influence soil physicochemical properties and microbial function in a semi-arid woodland ecosystem. *Plant and Soil* 456: 43-59
16. Fang O, Zhang QB (2019) Tree resilience to drought increases in the Tibetan Plateau. *Global change biology* 25(1): 245-253
17. Farquhar GD, Lloyd J (1993) Carbon and oxygen isotope effects in the exchange of carbon dioxide between terrestrial plants and the atmosphere. In *Stable isotopes and plant carbon-water relations*. Academic Press 47-70
18. Feeley KJ, Daniel Zuleta (2022) Changing forests under climate change. *Nature plants* 8(9): 984-985
19. Gao S, Liu R, Zhou T, Fang W, Yi C, Lu R, Luo H (2018) Dynamic responses of tree-ring growth to multiple dimensions of drought. *Global Change Biology* 24(11): 5380-5390
20. Gao Y, Shi Y, Wang Q (2020) Seismic anisotropy in the southeastern margin of the Tibetan Plateau and its deep tectonic significances. *Chinese Journal of Geophysics* 63(3): 802-816
21. Gartner K, Nadezhdina N, Englisch M, Čermak J, Leitgeb E (2009) Sap flow of birch and Norway spruce during the European heat and drought in summer 2003. *Forest Ecology and Management* 258(5): 590-599
22. Ge F, Sielmann F, Zhu X, Fraedrich K, Zhi X, Peng T, Wang L (2017) The link between Tibetan Plateau monsoon and Indian summer precipitation: a linear diagnostic perspective. *Climate dynamics* 49: 4201-4215
23. Gessler A, Ferrio JP, Hommel R, Treydte K, Werner RA, Monson RK (2014) Stable isotopes in tree rings: towards a mechanistic understanding of isotope fractionation and mixing processes from the leaves to the wood. *Tree physiology* 34(8): 796-818
24. Gessler A, Ferrio JP, Hommel R, Treydte K, Werner RA, Monson RK (2014) Stable isotopes in tree rings: towards a mechanistic understanding of isotope fractionation and mixing processes from the leaves to the wood. *Tree physiology* 34(8): 796-818.
25. Giraldo JA, Valle JI, González-Caro S, Sierra CA (2022) Intra-annual isotope variations in tree rings reveal growth rhythms within the least rainy season of an ever-wet tropical forest. *Trees* 36(3): 1039-1052
26. Griebinger J, Bräuning A, Helle G, Schleser GH, Hochreuther P, Meier W JH, Zhu H (2019) A dual stable isotope approach unravels common climate signals and species-specific responses to environmental change stored in multi-century tree-ring series from the Tibetan plateau. *Geosciences* 9(4): 151
27. Grossiord C, Sevanto S, Dawson TE, Adams HD, Collins AD, Dickman LT, McDowell NG (2017) Warming combined with more extreme precipitation regimes modifies the water sources used by trees. *New Phytologist*, 213(2): 584-596
28. Guo X, Tian L (2022) Spatial patterns and possible mechanisms of precipitation changes in recent decades over and around the Tibetan Plateau in the context of intense warming and weakening winds. *Climate Dynamics* 59(7-8): 2081-2102
29. Hahm WJ, Dralle DN, Rempe DM, Bryk AB, Thompson SE, Dawson TE, Dietrich W E (2019) Low subsurface water storage capacity relative to annual rainfall decouples Mediterranean plant productivity and water use from rainfall variability. *Geophysical Research Letters* 46(12): 6544-6553
30. Holdo RM, Nippert JB, Mack MC (2018) Rooting depth varies differentially in trees and grasses as a function of mean annual rainfall in an African savanna. *Oecologia* 186: 269-280
31. Hsieh JC, Chadwick OA, Kelly EF, Savin SM (1998) Oxygen isotopic composition of soil water: quantifying evaporation and transpiration. *Geoderma*, 82(1-3): 269-293
32. Hu H, Zhu L, Li H, X D, Xie Y (2021) Seasonal changes in the water-use strategies of three herbaceous species in a native desert steppe of Ningxia, China. *Journal of Arid Land* 13: 109-122.
33. Hu S, Zhou T, Wu B (2021) Impact of developing ENSO on Tibetan Plateau summer rainfall. *Journal of Climate* 34(9): 3385-3400
34. Huang R, Zhu H, Griebinger J, Wernicke J, Yu W, Bräuning A (2019) Temperature signals in tree-ring oxygen isotope series from the northern slope of the Himalaya. *Earth and planetary science letters* 506: 455-465
35. Jung M, Reichstein M, Schwalm CR, Huntingford C, Sitch S, Ahlström A, Zeng N (2017) Compensatory water effects link yearly global land CO₂ sink changes to temperature. *Nature* 541(7638): 516-520
36. Keyimu M, Li Z, Liu G, Fu B, Fan Z, Wang X, Halik U (2021) Tree-ring based minimum temperature reconstruction on the southeastern Tibetan Plateau. *Quaternary Science Reviews* 251: 106712

37. Li FF, Lu HL, Wang GQ, Yao ZY, Li Q, Qiu, J (2022) Zoning of precipitation regimes on the Qinghai–Tibet Plateau and its surrounding areas responded by the vegetation distribution. *Science of The Total Environment* 838: 155844
38. Li Q, Liu Y, Nakatsuka T, Fang K, Song H, Liu R, Wang K (2019) East Asian Summer Monsoon moisture sustains summer relative humidity in the southwestern Gobi Desert, China: Evidence from $\delta^{18}\text{O}$ of tree rings. *Climate dynamics* 52: 6321-6337.
39. Li Y, Peng S, Liu H, Zhang X, Ye W, Han Q, Li Y (2020) Westerly jet stream controlled climate change mode since the Last Glacial Maximum in the northern Qinghai-Tibet Plateau. *Earth and Planetary Science Letters* 549: 116529
40. Lind, Zhang, L, Falste D, Franklin O, Brännström A (2014) Plant diversity and drought: The role of deep roots. *Ecological modelling* 290: 85-93
41. Liu X, Liu, Y, Wang X, Wu G (2021) Large-scale dynamics and moisture sources of the precipitation over the western Tibetan Plateau in boreal winter. *Journal of Geophysical Research: Atmospheres* 125(9): e2019JD032133
42. Liu Y, An Z, Linderhol HW, Chen D, Song H, Cai Q, Tian, H (2009) Annual temperatures during the last 2485 years in the mid-eastern Tibetan Plateau inferred from tree rings. *Science in China Series D: Earth Sciences*: 52(3), 348-359
43. Liu Y, Wu G, Hong J, Dong B, Duan A, Bao Q, Zhou L (2012) Revisiting Asian monsoon formation and change associated with Tibetan Plateau forcing: II. Change. *Climate dynamics* 39: 1183-1195
44. Lloyd J, Farquhar GD (1994) ^{13}C discrimination during CO_2 assimilation by the terrestrial biosphere. *Oecologia* 99: 201-215
45. Ma J, Han J, Zhang Y, Dong Q., Lei N., Liu Z., Du Y (2020) Temporal stability of soil water content on slope during the rainy season in gully regulation watershed. *Environmental Earth Sciences* 79(8):173
46. McCarroll D, Load NJ (2004) Stable isotopes in tree rings. *Quaternary Science Reviews* 23(7-8): 771-801
47. Mirfenderesgi G, Bohrer G, Matheny AM, Fatichi S, Schäfer KV (2016) Tree level hydrodynamic approach for resolving aboveground water storage and stomatal conductance and modeling the effects of tree hydraulic strategy. *Journal of Geophysical Research: Biogeosciences* 121(7): 1792-1813
48. Murray FW (1966) On the computation of saturation vapor pressure. *Rand Corp Santa Monica Calif*
49. Nakawatase JM, Peterson DL (2006) Spatial variability in forest growth–climate relationships in the Olympic Mountains, Washington. *Canadian Journal of Forest Research* 36(1): 77-91
50. Ne M, Hulme M, Jones P (1999) Representing twentieth-century space–time climate variability. Part I: Development of a 1961–90 mean monthly terrestrial climatology. *Journal of climate* 12(3): 829-856
51. Nolan RH, Tarin T, Rumman R, Cleverly J, Fairweather KA, Zolfagha S, Eamus D (2018) Contrasting ecophysiology of two widespread arid zone tree species with differing access to water resources. *Journal of Arid Environments* 153: 1-10
52. Oerter E, Finstad K, Schaefer J, Goldsmith GR, Dawson T, Amundson R (2014) Oxygen isotope fractionation effects in soil water via interaction with cations (Mg, Ca, K, Na) adsorbed to phyllosilicate clay minerals. *Journal of Hydrology* 515: 1-9
53. Priyadarshini KVR, Prins HH, de Bie S, Heitkönig IM, Woodborne S, Gort G, de Kroon H (2016) Seasonality of hydraulic redistribution by trees to grasses and changes in their water-source use that change tree–grass interactions. *Ecohydrology* 9(2): 218-228
54. Rao W, Chen X, Meredith KT, Tan H, Gao M, Liu J (2020) Water uptake of riparian plants in the lower Lhasa River Basin, South Tibetan Plateau using stable water isotopes. *Hydrological Processes* 34(16): 3492-3505
55. Roden JS, Johnstone JA, Dawson TE (2011) Regional and watershed-scale coherence in the stable-oxygen and carbon isotope ratio time series in tree rings of coast redwood (*Sequoia sempervirens*). *Tree-Ring Research* 67(2): 71-86
56. Roden JS, Lin G, Ehleringer JR (2000) A mechanistic model for interpretation of hydrogen and oxygen isotope ratios in tree-ring cellulose. *Geochimica et Cosmochimica Acta* 64(1): 21-35
57. Schwendenmann L, Pendall E, Sanchez-Bragado R, Kunert N, Hölscher D (2015) Tree water uptake in a tropical plantation varying in tree diversity: interspecific differences, seasonal shifts and complementarity. *Ecohydrology* 8(1): 1-12
58. Seddon AW, Macias-Fauria M, Long PR, Benz D, Willis KJ (2016) Sensitivity of global terrestrial ecosystems to climate variability. *Nature* 531(7593): 229-232
59. Seneviratne SI, Corti T, Davin EL, Hirschi M, Jaeger EB, Lehner I, Teuling AJ (2010) Investigating soil moisture–climate interactions in a changing climate: A review. *Earth-Science Reviews* 99(3-4): 125-161
60. Shi PJ, Huang JG, Hui C, Grissino-Mayer, HD, Tardif J, Zhai LH, Li BL (2015) Capturing spiral radial growth of conifers using the superellipse to model tree-ring geometric shape. *Frontiers in plant science* 6: 856
61. Sidorova OV, Siegwolf RT, Saurer M, Shashkin AV, Knorre AA, Prokushkin AS, Kirydanov AV (2009) Do centennial tree-ring and stable isotope trends of *Larix gmelinii* (Rupr.) Rupr. indicate increasing water shortage in the Siberian north? *Oecologia* 161: 825-835
62. Sun L, Yang L, Chen L, Zhao F, Li S (2019) Short-term changing patterns of stem water isotopes in shallow soils underlain by fractured bedrock. *Hydrology Research* 50(2): 577-588
63. Sun J, Ye C, Liu M, Wang Y, Chen J, Wang S, Tsubo M (2022) Response of net reduction rate in vegetation carbon uptake to climate change across a unique gradient zone on the Tibetan Plateau. *Environmental research* 203: 111894

64. Su Zhou, T, Liu, Chen, Y, Shang H, Zhu L, Sha Y (2018) Linkages of the dynamics of glaciers and lakes with the climate elements over the Tibetan Plateau. *Earth-Science Reviews* 185: 308-324
65. Tan L, Cai Y, Cheng, Edwards LR, Lan J, Zhang H, Gao Y (2018) High resolution monsoon precipitation changes on southeastern Tibetan Plateau over the past 2300 years. *Quaternary Science Reviews*,195: 122-132
66. Van T, Verheyen K, Kint V, Van E, Muys B (2017) Plasticity of tree architecture through interspecific and intraspecific competition in a young experimental plantation. *Forest Ecology and Management* 385: 1-9
67. Wang H, Tetzlaff D, Soulsby C (2018) Modelling the effects of land cover and climate change on soil water partitioning in a boreal headwater catchment. *Journal of Hydrology*, 558: 520-531
68. Wang J, Taylor AR, D'Orangeville L (2023) Warming-induced tree growth may help offset increasing disturbance across the Canadian boreal forest. *Proceedings of the National Academy of Sciences*,120(2): e2212780120
69. Wan L, Liu H, Leavit S, Cresse EL, Quine TA, Shi J, Shi S (2021) Tree-ring $\delta^{18}\text{O}$ identifies similarity in timing but differences in depth of soil water uptake by trees in mesic and arid climates. *Agricultural and Forest Meteorology* 308: 108569
70. Wernicke J, Griebinger J, Hochreuther P, Bräuning A (2015) Variability of summer humidity during the past 800 years on the eastern Tibetan Plateau inferred from $\delta^{18}\text{O}$ of tree-ring cellulose. *Climate of the Past* 11(2): 327-337
71. Wong J, Fong A, McVicar N, Smith S, Giambattista J, Wells D, Alexander A (2020) Comparing deep learning-based auto-segmentation of organs at risk and clinical target volumes to expert inter-observer variability in radiotherapy planning. *Radiotherapy and Oncology* 144: 152-158
72. Wu G, Liu Y, Zhang Q, Duan A, Wang T, Wan R, Liang X (2007) The influence of mechanical and thermal forcing by the Tibetan Plateau on Asian climate. *Journal of Hydrometeorology* 8(4): 770-789
73. Wu H, Li XY, Zhang J, Li J, Liu J, Tian L, Fu C (2019) Stable isotopes of atmospheric water vapor and precipitation in the northeast Qinghai-Tibetan Plateau. *Hydrological Processes* 33(23): 2997-3009
74. Xiao H, Deng W, Wei G, Chen J, Zheng X, Shi T, Zeng T (2020) A pilot study on zinc isotopic compositions in shallow-water coral skeletons. *Geochemistry, Geophysics, Geosystems* 21(11): e2020GC009430
75. Xu C, Zhao Q, An W, Wang S, Tan N, Sano M, Guo Z (2021) Tree-ring oxygen isotope across monsoon Asia: Common signal and local influence. *Quaternary Science Reviews* 269: 107156
76. Xu C, Zhu H, Nakatsuka T, Sano M, Li Z, Shi F, Guo Z (2019) Sampling strategy and climatic implication of tree-ring cellulose oxygen isotopes of *Hippophae tibetana* and *Abies georgei* on the southeastern Tibetan Plateau. *International journal of biometeorology* 63: 679-686
77. Xu G, Liu X, Sun W, Szejner P, Zeng X, Yoshimura K, Trouet (2020). Seasonal divergence between soil water availability and atmospheric moisture recorded in intra-annual tree-ring $\delta^{18}\text{O}$ extremes. *Environmental Research Letters* 15(9): 094036
78. Xu G, Wu G, Liu X, Chen T, Wang B, Hudson A, Trouet V (2020) Age-related climate response of tree-ring $\delta^{13}\text{C}$ and $\delta^{18}\text{O}$ from spruce in northwestern China, with implications for relative humidity reconstructions. *Journal of Geophysical Research: Biogeosciences*: 125(7): e2019JG005513
79. Xu Q, Li H, Chen J, Cheng X, Liu S, An S (2011) Water use patterns of three species in subalpine forest, Southwest China: the deuterium isotope approach. *Ecohydrology* 4(2): 236-244
80. Yang B, Wen X, Sun X (2015) Seasonal variations in depth of water uptake for a subtropical coniferous plantation subjected to drought in an East Asian monsoon region. *Agricultural and Forest Meteorology* 201: 218-228
81. Yao Y, Liu Y, Zhou S, Son J, Fu B (2023) Soil moisture determines the recovery time of ecosystems from drought. *Global Change Biology* 29(13): 3562-3574
82. Young GH, Loader NJ, McCarroll D, Bale RJ, Demmler JC, Miles D, Whitney M (2015) Oxygen stable isotope ratios from British oak tree-rings provide a strong and consistent record of past changes in summer rainfall. *Climate Dynamics* 45: 3609-3622
83. Zeng Q, Rossi S, Yang B, Qin C, Li G (2020) Environmental drivers for cambial reactivation of *Qilian junipers* (*Juniperus przewalskii*) in a semi-arid region of northwestern China. *Atmosphere* 11(3): 232
84. Zeng X, Li X, Evans MN, Wang W, An W, Xu G, Wu G (2016) Seasonal incursion of Indian Monsoon humidity and precipitation into the southeastern Qinghai-Tibetan Plateau inferred from tree ring $\delta^{18}\text{O}$ values with intra-seasonal resolution. *Earth and Planetary Science Letters* 443: 9-19
85. Zhan N, Wang Z, Xie Y, Shang X, Liu G, Wu Z (2021) Expression patterns and regulation of non-coding RNAs during synthesis of cellulose in *Eucalyptus grandis* Hill. *Forests* 12(11): 1565
86. Zhang F, Jia W, Zhu G, Shi Y, Zhang M (2022) Using stable isotopes to investigate differences of plant water sources in subalpine habitats. *Hydrological Processes* 36(2): e14518
87. Zhang J, Gou X, Alexander MR, Xia J, Wang F, Zhang F, Pederson N (2021) Drought limits wood production of *Juniperus przewalskii* even as growing seasons lengthens in a cold and arid environment. *Catena* 196: 104936

88. Zhang J, Gou X, Manzanedo RD, Zhang F, Pederson N (2018) Cambial phenology and xylogenesis of *Juniperus przewalskii* over a climatic gradient is influenced by both temperature and drought. *Agricultural and forest meteorology* 260: 165-175
89. Zhou Y, Chen S, Song W, Lu Q, Lin G (2011) Water-use strategies of two desert plants along a precipitation gradient in northwestern China. *Chinese Journal of Plant Ecology* 35(8): 789-80

Figures

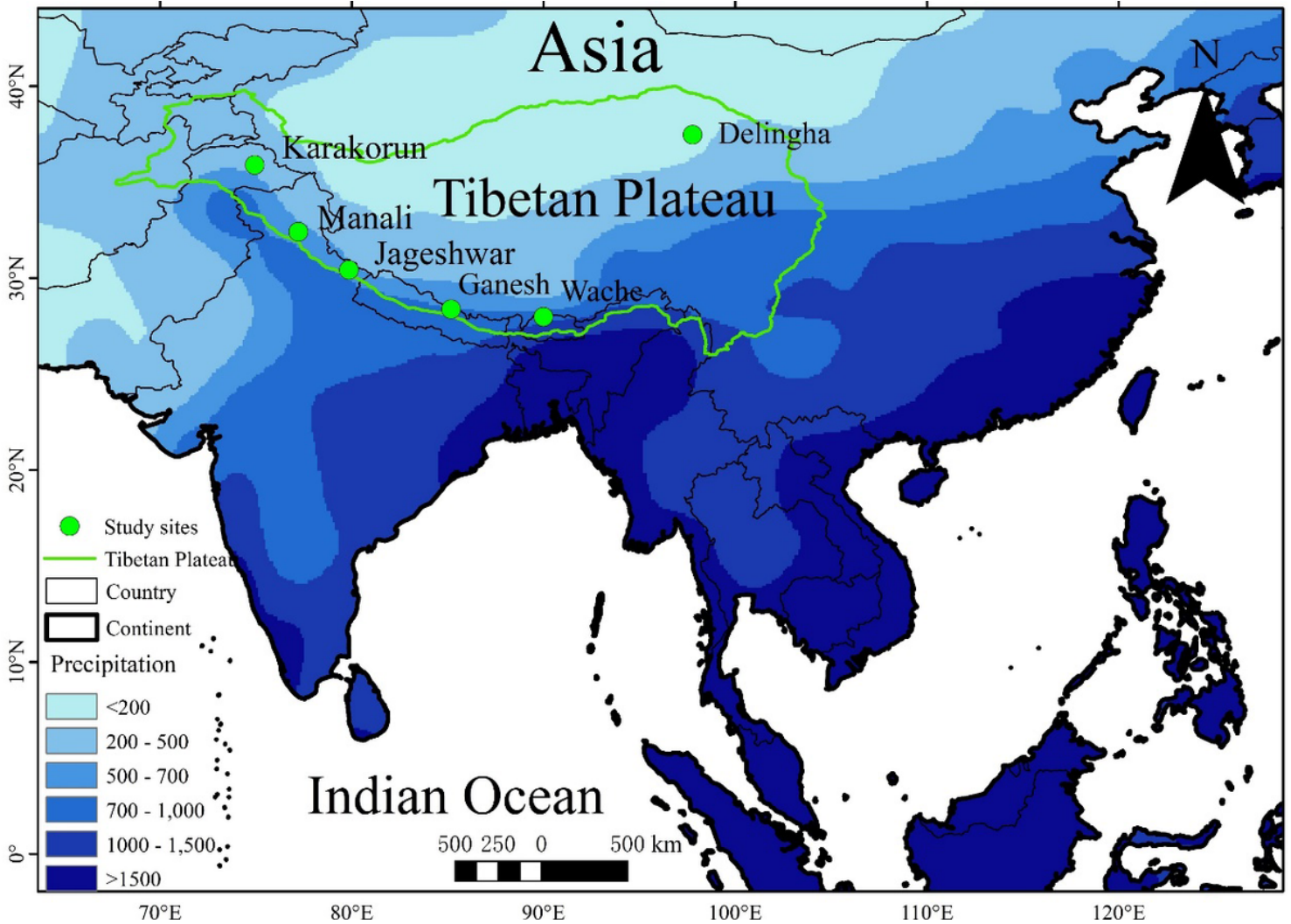


Figure 1
 Geographical locations of study area and sampling sites. The green line in the figure represents the boundary line of the Tibetan Plateau, the green dots are the tree wheel sampling points, the different shades of blue represent the different amounts of rainfall in the region, and the darker the color means more precipitation.

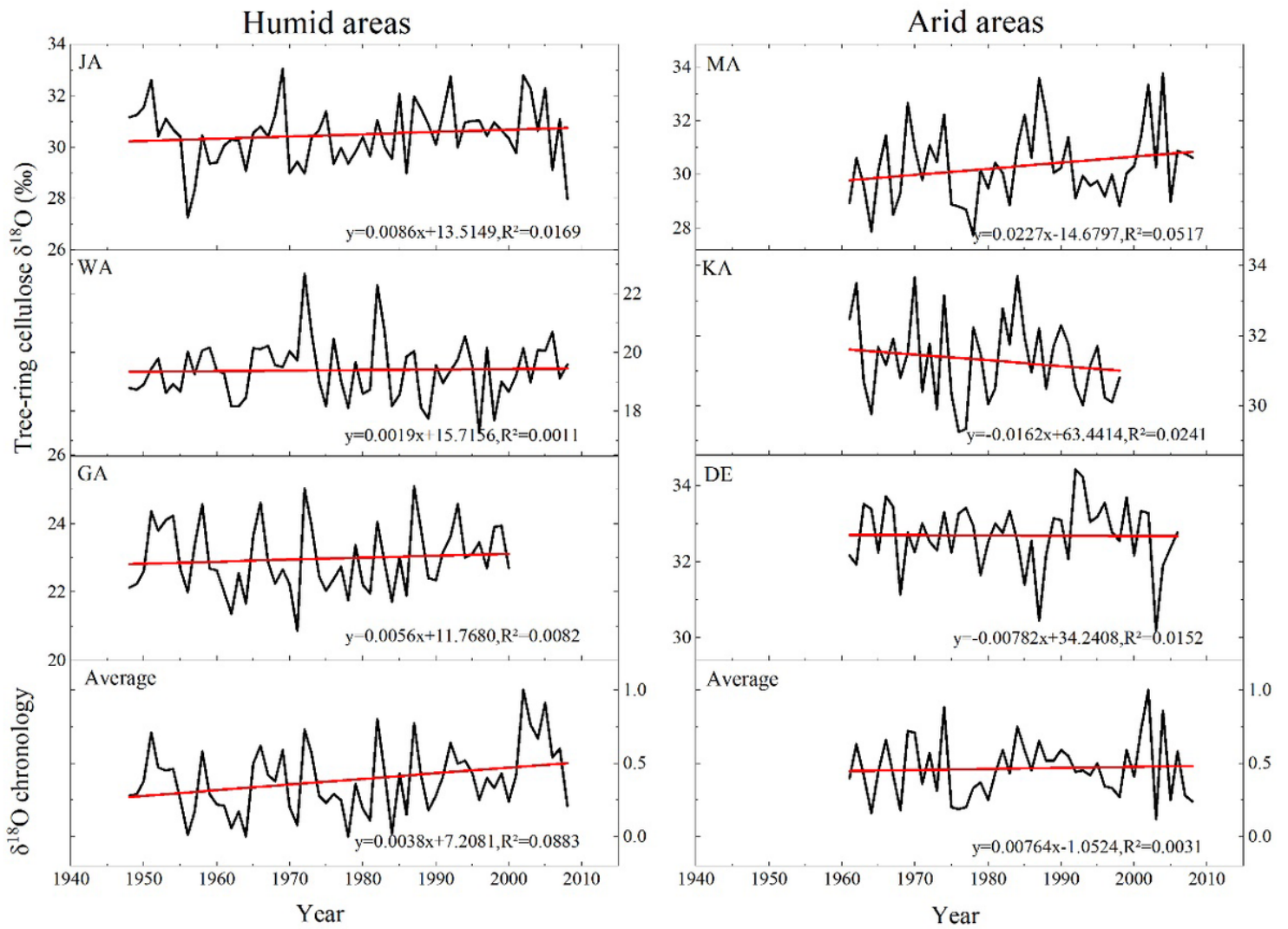


Figure 2

The time series of the $\delta^{18}O_{TR}$ for each site. The red solid line indicates the trend for each chronology.

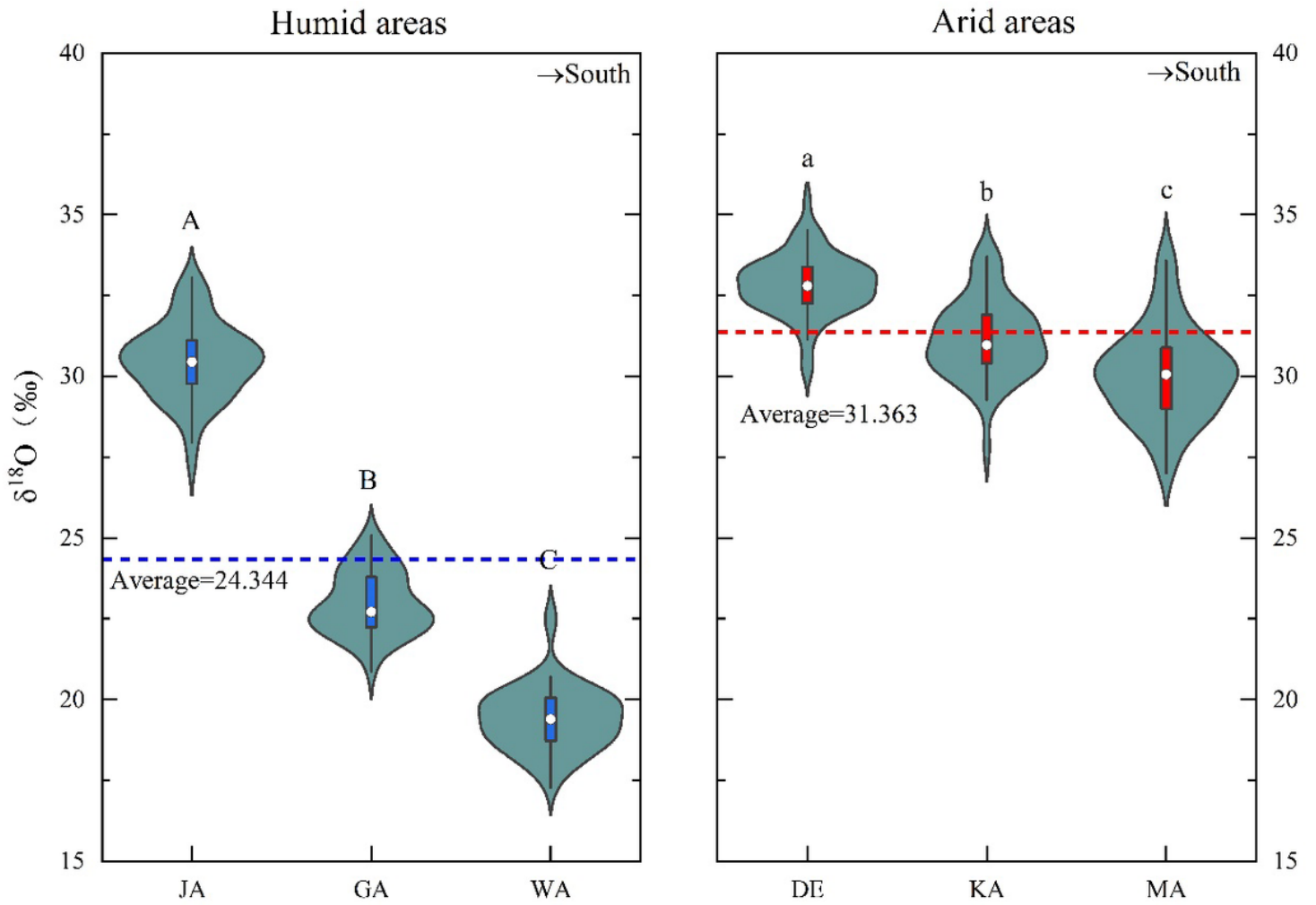


Figure 3

Significance test for study sites. The box in the figure represents the average value of $\delta^{18}\text{O}_{\text{TR}}$ for each point from 1948 to 1998. Inter-sample differences in $\delta^{18}\text{O}_{\text{TR}}$ values were assessed using one-way ANOVA, with different letters indicating significant differences at the 0.05 confidence level. And the red dashed line represents the mean value of $\delta^{18}\text{O}_{\text{TR}}$ in the arid areas and the blue dashed line represents the mean value of $\delta^{18}\text{O}_{\text{TR}}$ in the humid areas.

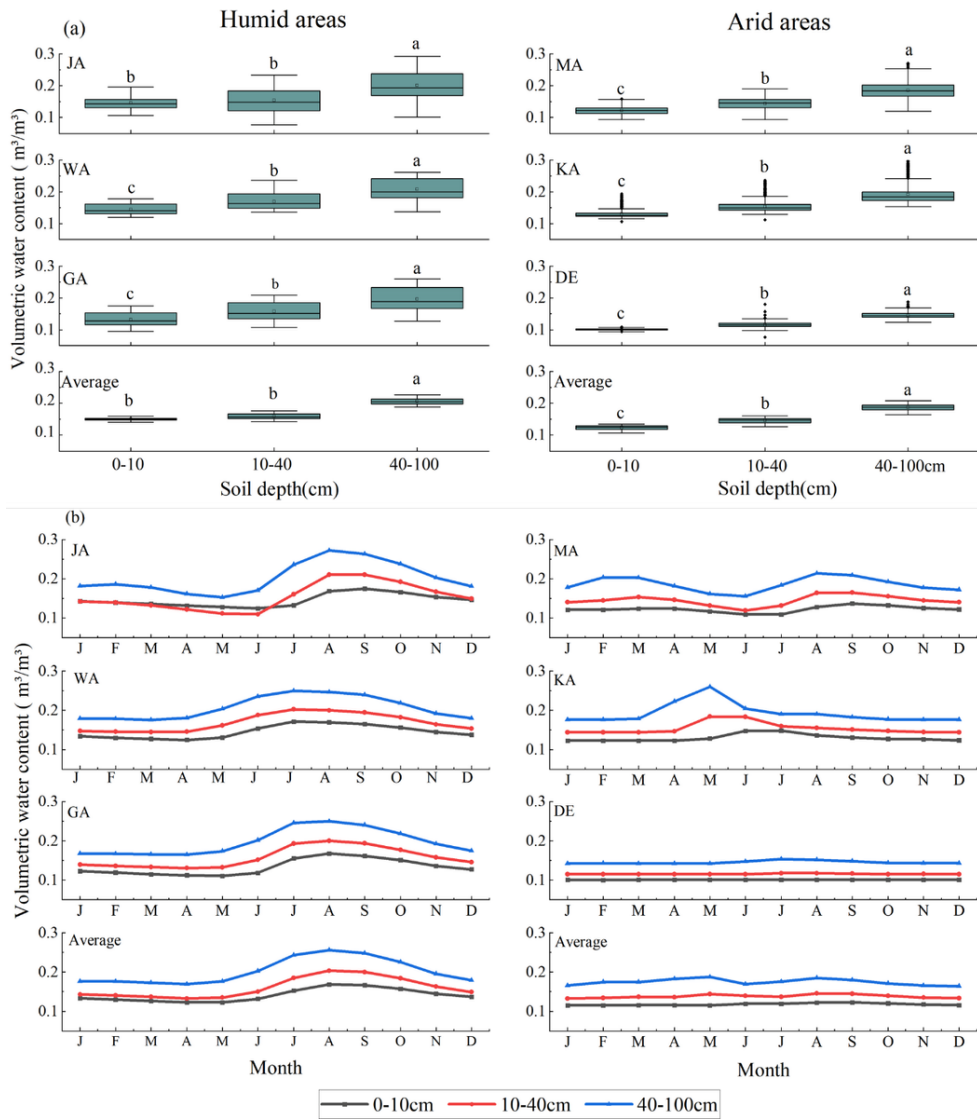


Figure 4

Changes of soil moisture at different soil layers and annual scales. The squares in the box line diagram represent the median volumetric water content, the black dots represent the outliers and the range of the boxes represents the 25%-75% data interval (a). The blue line in the graph represents the 40-100 cm volumetric water content, the red line represents the 10-40 cm volumetric water content and the black line represents the 0-10 cm volumetric water content (b).

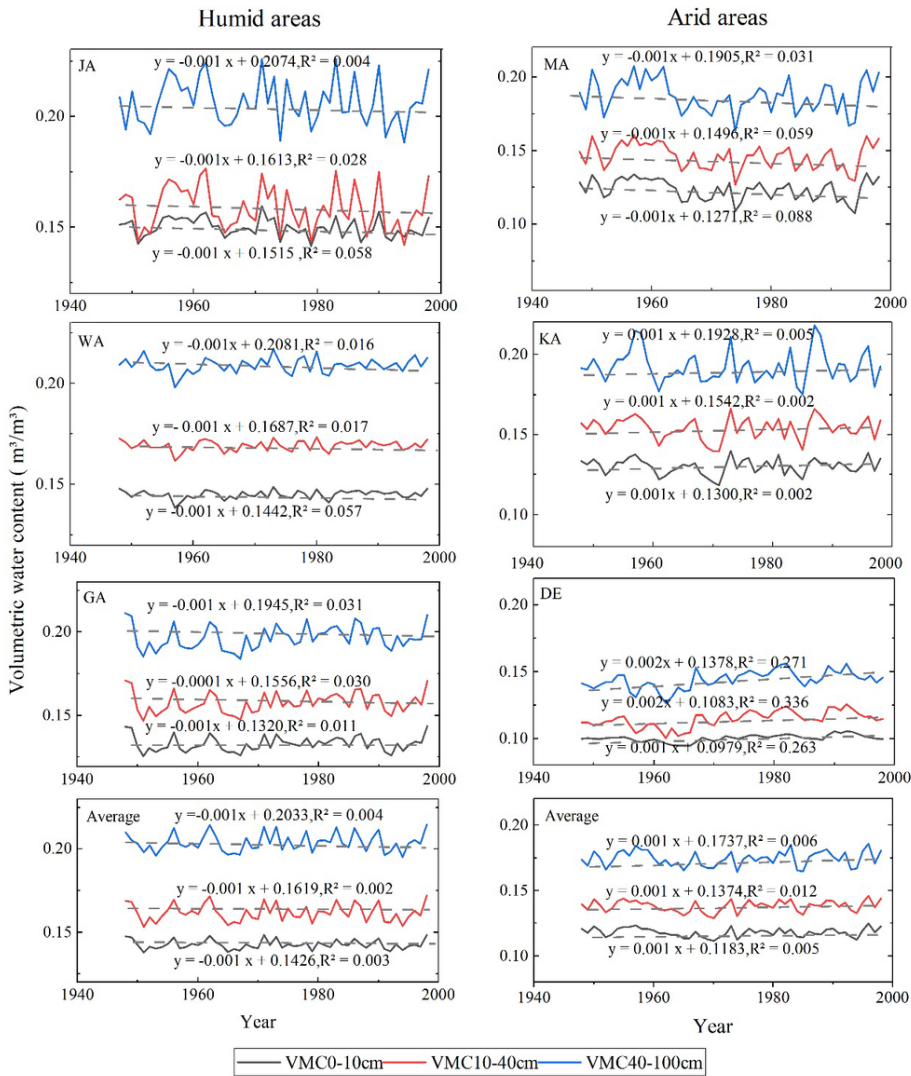


Figure 5

Interannual variation of soil moisture. The blue line represents 40-100cm volumetric water content, the red line represents 10-40cm volumetric water content, the black line represents 0-10cm volumetric water content, and the grey dashed line represents the trend line.

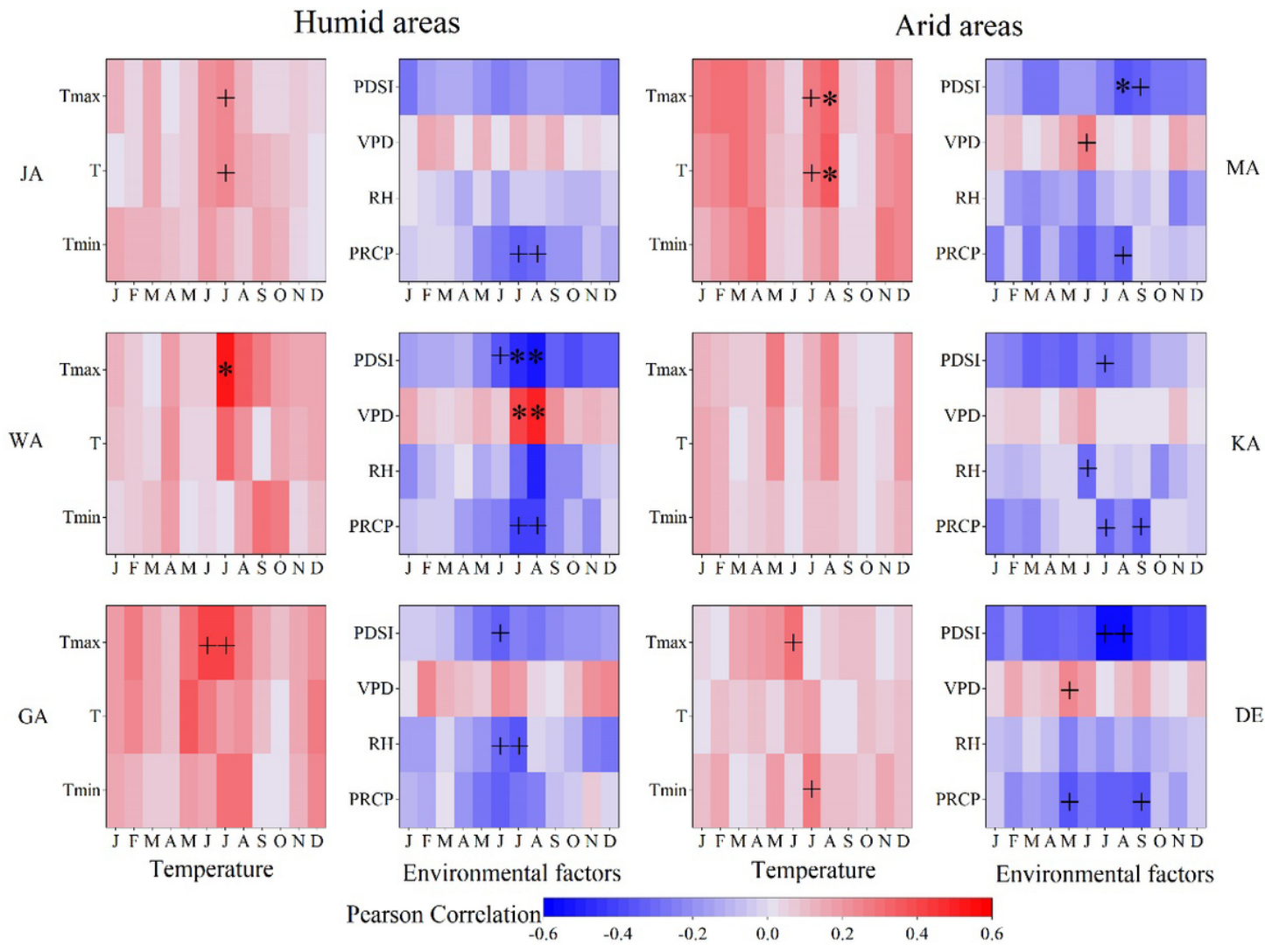


Figure 6

Correlations of $\delta^{18}\text{O}_{\text{TR}}$ with monthly climate variables (temperature, PDSI, VPD, RH, PRCP). The "+" and "*" indicate significant correlations at the 95% and 99% level, respectively. The Tmax stands for maximum temperature, T stands for mean temperature, the Tmin stands for minimum temperature, PDSI stands for Palmer Drought Index, VPD stands for vapor pressure deficit, RH stands for relative humidity, PRCP stands for precipitation.

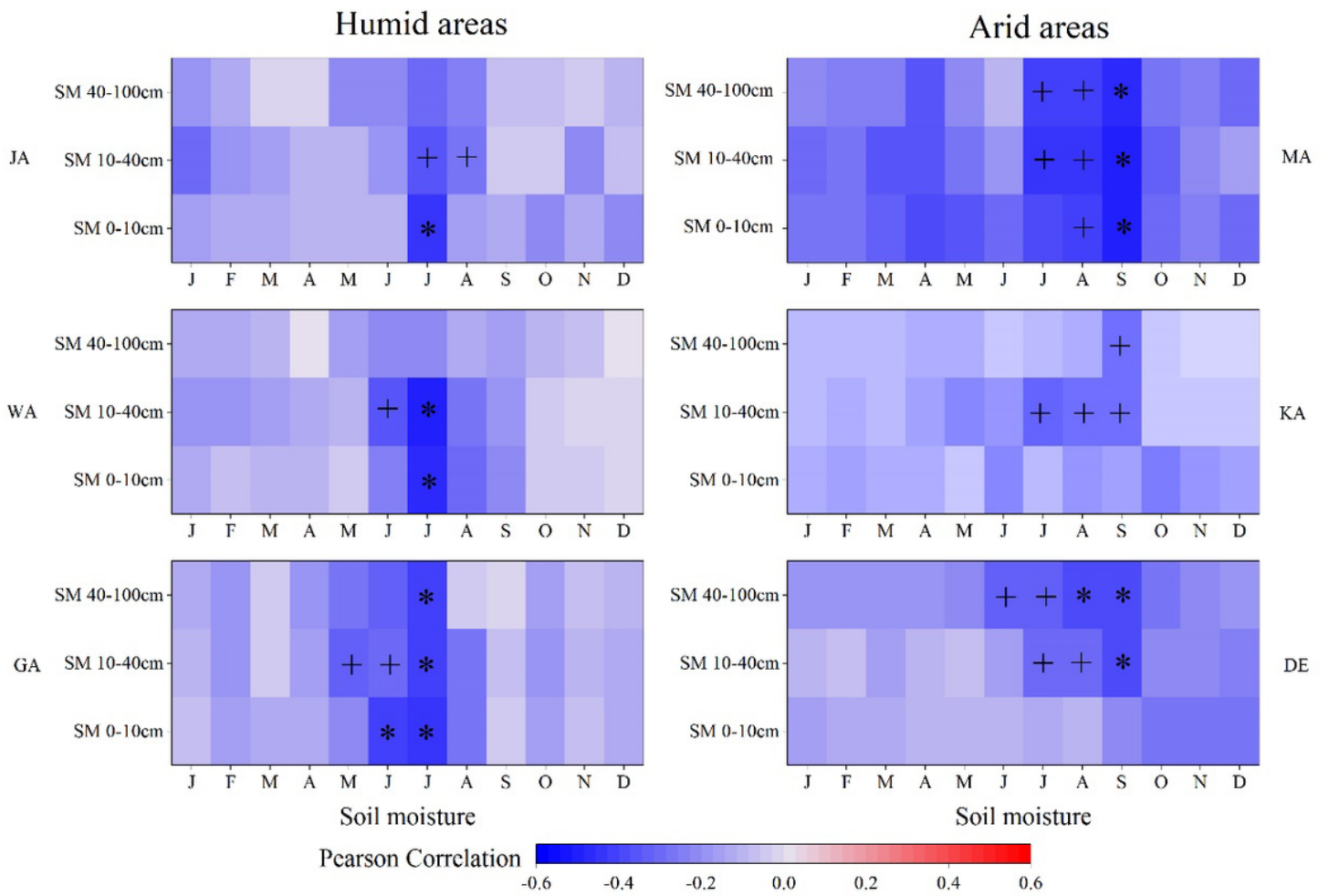


Figure 7

Correlations of $\delta^{18}\text{O}_{\text{TR}}$ with monthly soil moisture. The "+" represents $p < 0.05$, "*" represents $p < 0.01$, SM40-100 cm represents 40-100 cm soil moisture, SM10-40 cm represents 10-40 cm soil moisture, SM0-10 cm represents 0-10 cm soil moisture.

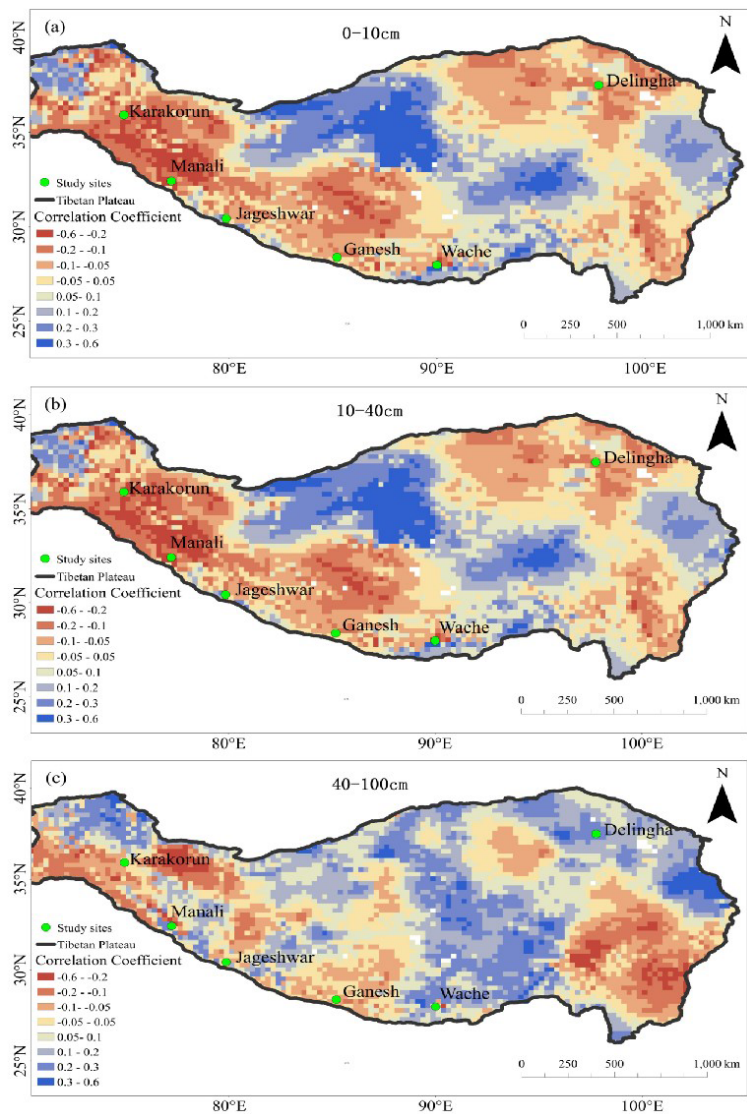


Figure 8

The spatial correlation between the June-September VWC in each soil layer and $\delta^{18}\text{O}_{\text{TR}}$. The green point in the figure represents $\delta^{18}\text{O}_{\text{TR}}$ sampling points and the black line is the Tibetan Plateau boundary line.

Supplementary Files

This is a list of supplementary files associated with this preprint. Click to download.

- [Appendix.docx](#)